Journal of Materials Processing Tech. 261 (2018) 159–163

Contents lists available at ScienceDirect

Journal of Materials Processing Tech.

journal homepage: www.elsevier.com/locate/jmatprotec

Effect of stirring rate on microstructure and properties of microporous mullite ceramics

Wenfeng Li[a,*], Huishi Guo[b,*], Qingfei Huang[a], Ping Han[a], Yonggai Hou[a], Wenjun Zou[a]

[a] School of Materials Science and Engineering, Henan University of Technology, Zhengzhou 450001, China
[b] School of Materials and Chemical Engineering, Zhengzhou University of Light Industry, Zhengzhou 450001, China

ARTICLE INFO

Keywords:
Porous ceramics
Foaming
Stirring rate
Bubble generation
Bubble splitting
Properties

ABSTRACT

When suspensions are stirred at low stirring rates (400–800 rpm), microporous mullite ceramics with high bulk density and low apparent porosity can be achieved because the content of bubbles in suspensions is scarce. With the stirring rate increases from 1200 rpm to 2000 rpm, more and larger bubbles are generated in suspensions. Under actions of the force from spinning blades and the shear stress from adjacent flow layers, these larger bubbles are divided into smaller ones and dispersed evenly, which is helpful to reduce the bulk density and thermal conductivity of as-prepared ceramics. When the stirring rate increases up to 2400 rpm, bubble structures are easily destroyed because some suspensions are thrown out of the mixer by the excessive force of blades, which lead to increases in the bulk density, crushing strength and thermal conductivity.

1. Introduction

Zhao et al. (2015) used sacrificial template to produce honeycomb SnO_2 foams. Xu et al. (2015) obtained porous alumina ceramics by a precipitation method. Subhasree et al. (2016) fabricated $ZrTiO_4$-TiO_2 porous ceramics via direct foaming. Guo et al. (2015) stated that the direct foaming method is suitable for producing porous ceramics with low bulk density, small-sized and closed pores. Tian and Ma (2012) introduced this method in detail, showing that numerous air bubbles are generated in aqueous solutions of ceramic powders by mechanical stirring, they transform into pores in ceramics after consolidating, drying and sintering. If the stirring rate is too slow, the amount of air bubbles generated in suspensions, as well as the splitting effect on these bubbles, will be limited because the force of revolving blades is weak. On the contrary, if the stirring rate is too fast, bubble structures in suspensions will be destroyed due to the excessive power of revolving blades. It is a very significant and valuable work to study the stirring rate of blades in suspensions for preparation of high-performance porous ceramics with tailored porous structures by foaming. Most of researches on the direct foaming method are mainly focused on studying the kind and content of foaming agents as reported by Yin et al. (2013), the optimization of solid loading as described by Dong et al. (2017) and the solidifying technology of foamed suspensions as reported by Yoon et al. (2010), while there are few reports on this aspect.

In this study, microporous mullite ceramics are prepared by direct foaming method. The microstructure and performance (including apparent porosity, bulk density, crushing strength, pore size distribution and thermal conductivity) of microporous mullite ceramics are studied as a function of the stirring rate of blades in suspensions.

2. Experimental procedure

2.1. Materials

Commercially available kyanite powder with an average particle diameter (d_{50}) of 75 μm and Al_2O_3 content of 53±1% was applied as the main starting material. $Al(OH)_3$ with d_{50} of 84 μm and Al_2O_3 content of 66.8±1% was chosen as the alumina source. Sodium dodecyl benzene sulfonate (SDBS, Chemical purity) was used as the foamer. The aluminate cement (AC) with d_{50} of 45 μm and Al_2O_3 content of 55% was selected as the coagulant of foamed suspensions.

2.2. Sample preparation

The powder mixture composed of 57 wt% kyanite, 38 wt% $Al(OH)_3$ and 5 wt% AC was dry mixed for 2 h. It was wet mixed for 3 min with deionized water at solid loading of 55 vol%. SDBS was added into the wet mixture at 0.4 wt% according to the solid mixture, followed by whisking at different stirring rates (400–2400 rpm, an interval of 400 rpm) for 5 min to get foamed suspensions. These suspensions were cast into polyethylene moulds with the size of

* Corresponding authors.
E-mail addresses: wenfengzly@163.com (W. Li), guohuishi@zzuli.edu.cn (H. Guo).

https://doi.org/10.1016/j.jmatprotec.2018.06.017
Received 31 March 2018; Received in revised form 12 June 2018; Accepted 13 June 2018
Available online 14 June 2018
0924-0136/

40 mm × 40 mm × 40 mm and cured at room temperature for 48 h. After demoulding, the green bodies were dried at 80 °C for 24 h with the heating rate of 1.5 °C/min and sintered in an electric furnace at a temperature of 1500 °C for 3 h in air.

2.3. Characterization

Phase composition of microporous mullite ceramics was identified by X-ray diffractometer (XRD, Panalytical X'pert) with CuKα radiation at 40 kV and 40 mA. Microstructure was characterised using a scanning electron microscopy (SEM, JEOL JSM-7600F). Mean pore size and pore size distribution were examined by mercury intrusion porosimetry in a Quantachrome PM-60GT instruments. Both apparent porosity and bulk density were tested in distilled water according to Archimedes method. Crushing strength was tested using a uniaxial crushing tester (HT-8391). Thermal conductivity at 1100 °C was determined using a flat plate thermo-conductivity tester (PBDR-02P). Three to five specimens were used to determine the average values of apparent porosity, bulk density, crushing strength and thermal conductivity.

3. Results and discussion

3.1. Phase composition and microstructure

Fig. 1 depicts XRD analysis results of the sample produced at 2000 rpm. It is found that the predominant crystalline phase in this sample is mullite (PDF#79-1454), accompanied with a small amount of corundum (PDF#71-1123). As Guo et al. (2016) and Ahmad et al. (2015) stated in their papers, some of mullites come from the mullitization of kyanite, namely primary mullite. The others come from the reaction between Al_2O_3 (decomposition of $Al(OH)_3$) and silica in the glassy phase, namely secondary mullite. The existed corundum is ascribed to the excess Al_2O_3 in as-synthesized secondary mullite. These can be understood in terms of reactions by following equations:

$$2Al(OH)_3 \xrightarrow{198-570^{\circ}C} Al_2O_3 + 3H_2O \quad (1)$$

$$3(Al_2O_3{\cdot}SiO_2)(kyanite) \xrightarrow{1100-1300^{\circ}C} 3Al_2O_3{\cdot}2SiO_2(mullite) + SiO_2 \quad (2)$$

$$3Al_2O_3 + 2SiO_2 \xrightarrow{>1300^{\circ}C} 3Al_2O_3{\cdot}2SiO_2(mullite) \quad (3)$$

SEM images of samples under diverse stirring rates are displayed in Fig. 2, showing that the stirring rate of foamed suspensions has significant effects on the formation and evolution of pore size, number and distribution. When the stirring rate is 400–800 rpm (Fig. 2a and b), there are only a few small pores with thick walls, their size range is in the 20–60 μm. With increasing the stirring rate from 1200 rpm to 1600 rpm (Fig. 2c and d), the number of pores increases, and their size enlarges to about 50–150 μm. Meanwhile, their wall thickness becomes thinner. For the sample prepared at the stirring rate of 2000 rpm (Fig. 2e), more pores can be observed, these pores distribute uniformly and their size decreases to about 40–100 μm. When the stirring rate further increases up to 2400 rpm (Fig. 2f), the number of pores decreases and their size is up to 80–170 μm due to some neighbouring pores connecting with each other.

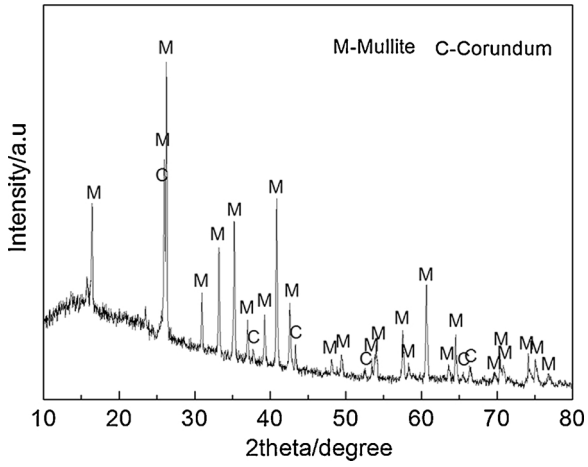

Fig. 1. XRD pattern of the sample produced at 2000 rpm.

When suspensions are stirred, the air is introduced into them. The SDBS which distributes uniformly in suspensions will be adsorbed on the air-liquid interface. Its hydrophobic parts are expelled from the solvent and the hydrophilic parts remain in contact with the liquid, which results in lower the surface tension of air-liquid interface and make air bubbles generate. These air bubbles suffer not only the force from revolving blades, but also the shear stress from adjacent flow layers. As shown in Fig. 3, there is a turbulent shear stress τ between flow layers I andII. When the value of τ is higher than that of the surface tension of bubble films, large bubbles will be divided into smaller and independent ones.

Fig. 4 illustrates the schematic drawing of bubble splitting in flow fields. It can be seen that if there is no relative movement between two adjacent flow layers, the bubble will stay in the middle of them and maintain its original state (Fig. 4a). Once a relative movement exists between these two flow layers, the turbulent shear stress τ will generate, which makes the bubble divide into smaller ones (Fig. 4b). As the relative displacement between two adjacent flow layers increases, these smaller bubbles can move along flow layers (Fig. 4c). When the value of τ is larger than that of the surface tension of bubble films, the smaller bubbles will be separated into independent ones (Fig. 4d). These independent bubbles can be captured by other tangent flow layers and are split until the τ cannot divide them in further, then bubbles in foamed suspensions are achieved.

When the stirring rate is 400–800 rpm, the amount of air introduced into suspensions is less because the revolving vortex formed in suspensions is small and bubbles are difficult to nucleate, which results in less and finer pores. With increasing stirring rate from 1200 rpm to 1600 rpm, more air will be incorporated into suspensions, the amount and size of bubbles generated in suspensions become more and larger, which lead to increases in the number and size of pores. As the stirring rate increases to 2000 rpm, blades in suspensions are gradually exposed to the atmosphere, the negative pressure zones are formed behind them, which introduce more air into suspensions and produce more bubbles. Under actions of the force from spinning blades and the shear stress from adjacent flow layers, larger bubbles are divided into smaller ones and disperse uniformly. All these factors contribute to reducing the pore size and enhancing the homogeneous distribution of pores. When the stirring rate increases up to 2400 rpm, some suspensions are easily spilled out of the mixer due to the excessively mixing power of rotating blades, bubble structures coalesce partially and then collapse, which result in less and larger pores.

3.2. Pore size distribution

Fig. 5 illustrates the pore size distribution of microporous mullite ceramics fabricated under various stirring rates, showing that it has a close relationship with the stirring rate of suspensions. For the sample prepared at the stirring rate of 400 rpm, the pore size distribution curve shows a unimodal characteristic. When the stirring rate increases, the number of characteristic peaks and the distribution range of pore sizes enlarge. Moreover, mean pore sizes of microporous mullite ceramics fabricated at various stirring rates increase firstly and then decrease. When the stirring rates are 400 rpm, 800 rpm, 1200 rpm, 1600 rpm, 2000 rpm and 2400 rpm, their values are 1.8 μm, 2.5 μm, 7.7 μm, 9.1 μm, 8.7 μm and 10.1 μm, respectively. From Fig. 2, it can be observed that the size of pores is in the range of 20–170 μm, it is obviously higher than the testing result from mercury porosimetry. Analysis of